

Tundra Greenness

<https://doi.org/10.25923/s86a-jn24>

**G. V. Frost¹, M. J. Macander¹, U. S. Bhatt², L. T. Berner³, J. W. Bjerke⁴,
H. E. Epstein⁵, B. C. Forbes⁶, M. J. Lara^{7,8}, R. Í. Magnússon⁹, P. M. Montesano¹⁰,
G. K. Phoenix¹¹, S. P. Serbin¹², H. Tømmervik⁴, C. Waigl¹³, D. A. Walker¹⁴,
and D. Yang^{12,15}**

¹Alaska Biological Research, Inc., Fairbanks, AK, USA

²Geophysical Institute, University of Alaska Fairbanks, Fairbanks, AK, USA

³School of Informatics, Computing and Cyber Systems, Northern Arizona University, Flagstaff, AZ, USA

⁴Norwegian Institute for Nature Research, FRAM - High North Research Centre for Climate and the Environment, Tromsø, Norway

⁵Department of Environmental Sciences, University of Virginia, Charlottesville, VA, USA

⁶Arctic Centre, University of Lapland, Rovaniemi, Finland

⁷Department of Plant Biology, University of Illinois, Urbana, IL, USA

⁸Department of Geography, University of Illinois, Urbana, IL, USA

⁹Plant Ecology and Nature Conservation Group, Wageningen University & Research, Wageningen, Netherlands

¹⁰Goddard Space Flight Center, NASA, Greenbelt, MD, USA

¹¹School of Biosciences, University of Sheffield, Sheffield, UK

¹²Environmental and Climate Sciences Department, Brookhaven National Laboratory, Upton, NY, USA

¹³International Arctic Research Center, University of Alaska Fairbanks, Fairbanks, AK, USA

¹⁴Institute of Arctic Biology, University of Alaska Fairbanks, Fairbanks, AK, USA

¹⁵Department of Ecology and Evolution, Stony Brook University, Stony Brook, NY, USA

Headlines

- The circumpolar average peak tundra greenness value in 2023 was the third highest in the 24-year MODIS record, a slight increase from the previous year.
- Peak vegetation greenness in 2023 was much higher than usual in North American tundra, particularly in the Beaufort Sea region, while greenness was relatively low in the Eurasian Arctic, particularly in north-central Siberia and the Russian Far Northeast.
- The eight highest circumpolar tundra greenness values in the long-term satellite record (1982-2022) have all been recorded in the last 12 years, providing unequivocal evidence of Arctic greening.

Introduction

Earth's northernmost continental landmasses and island archipelagos are home to the Arctic tundra biome, a 5.1 million km² region that forms a "ring" of cold-adapted, treeless vegetation atop the globe, bordered by the Arctic Ocean to the north and the boreal forest biome to the south (Raynolds et al. 2019). The biological and physical conditions of Arctic tundra ecosystems are changing profoundly, as vegetation and underlying permafrost soils are strongly influenced by rising air temperatures and the

rapid decline of sea ice on the nearby Arctic Ocean (see essays [Surface Air Temperature](#) and [Sea Ice](#)). In the late 1990s, a sharp increase in the productivity of tundra vegetation became evident in global satellite observations, a phenomenon that soon became known as “the greening of the Arctic.” Arctic greening is dynamically linked with Earth’s changing climate, permafrost, seasonal snow, and sea-ice cover, and remains a focus of multi-disciplinary scientific research.

Spaceborne monitoring of Arctic tundra greenness

Global vegetation has been monitored from space for over four decades, beginning with the launch of the Advanced Very High Resolution Radiometer (AVHRR) sensor in late 1981. In 2000, the Moderate Resolution Imaging Spectroradiometer (MODIS) began providing a complementary record with higher spatial resolution and improved calibration. AVHRR and MODIS both monitor vegetation greenness using the Normalized Difference Vegetation Index (NDVI), a spectral metric that exploits the unique way in which vegetation absorbs and reflects light in the visible and infrared wavelengths, respectively.

Both AVHRR and MODIS have recorded increasing annual maximum tundra greenness (MaxNDVI) across most of the Arctic tundra biome during 1982-2022 and 2000-23, respectively (Figs. 1a,b). Although there is substantial regional variability in greenness trends, several areas of strong positive trend stand out in both records. In North America, greening has been strongest in northern Alaska, mainland Canada, and southern Baffin Island. In Eurasia, strong greening has occurred in Chukotka and portions of the Taymyr Peninsula. However, some Arctic tundra regions have experienced flat or negative (sometimes referred to as “browning”) trends, including portions of southwestern Alaska, the Canadian High Arctic, and northeastern Siberia. Trends in northwestern Siberia and the European Arctic are mixed between the two satellite records, which may be partly attributable to their different observational periods. Regional contrasts in greening highlight the complexity of Arctic change, and the rich web of interactions that exist between tundra ecosystems and the local characteristics of sea ice, permafrost, seasonal snow (see essay [Terrestrial Snow Cover](#)), soil composition and moisture, disturbance processes, wildlife, and human activities (Bartsch et al. 2021; Heijmans et al. 2022). Parsing the underlying drivers of complex Arctic trends is important for improved monitoring and prediction of tundra ecosystem function and the consequences of Arctic change on the global carbon cycle (Rogers et al. 2022; see essay [Peatlands and Associated Boreal Forests of Finland Under Restoration](#)).

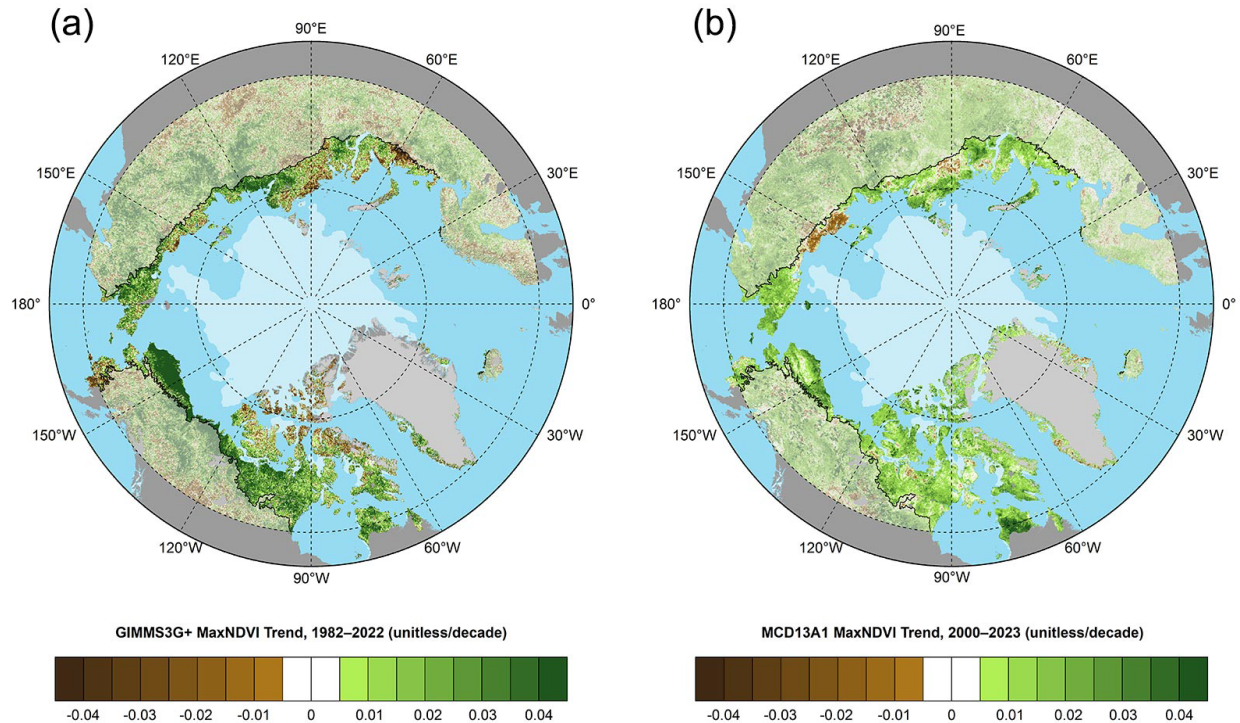


Fig. 1. Magnitude of the MaxNDVI trend calculated as the change per decade using ordinary least squares regression for Arctic tundra (solid colors), and boreal forest north of 60° latitude (muted colors) during (a) 1982-2022 based on the AVHRR GIMMS 3-g+ dataset, and (b) 2000-23 based on the MODIS MCD13A1 v6.1 dataset. In each panel, the circumpolar treeline is indicated by a black line, and the 15 August 2023 sea-ice extent is indicated by light shading.

The boreal forest biome (see Figs. 1a,b), which occupies large swaths of northern Eurasia and North America, has also emerged as a focal point of global environmental change. In this region, greening has generally prevailed along the forest-tundra ecotone in the north, whereas browning has been more frequent in the interior of the boreal forest biome (Berner and Goetz 2022). Patches of positive and negative greenness trends are widely interspersed, reflecting complex interactions among the biome's active wildfire regime, changing climate, extreme events, pathogens, and other factors (Foster et al. 2022).

In 2022—the most recent year with observations from both AVHRR and MODIS—circumpolar mean MaxNDVI for tundra regions was at or near record high values in both records. The AVHRR-observed MaxNDVI was the highest value on record (1982-2022), increasing 9.8% from 2021 (Fig. 2). Notably, the eight highest values in the 41-year AVHRR record have all been recorded within the last 12 years (i.e., 2011-22). The MODIS-observed circumpolar mean MaxNDVI value declined slightly (0.9%) from 2021 and was only 2.0% lower than the record high value observed in 2020. Circumpolar MaxNDVI trends derived from the two sensors are virtually identical for the period of overlap (2000-22), although the AVHRR record displays much higher variability, especially over the last 15 years. This is likely due in part to the lower spatial resolution and less advanced calibration of the AVHRR sensor compared to MODIS.

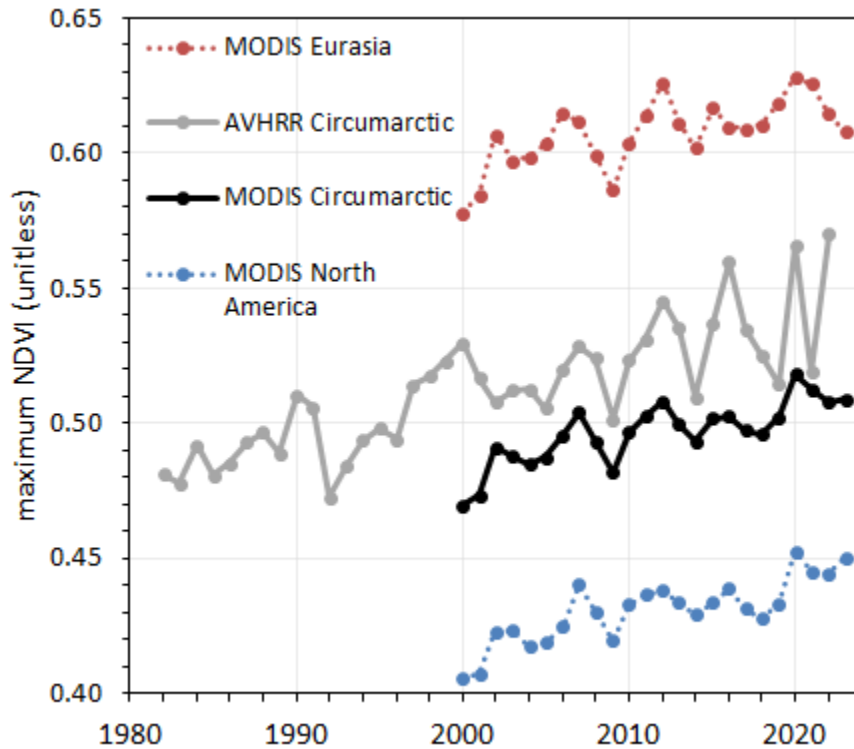
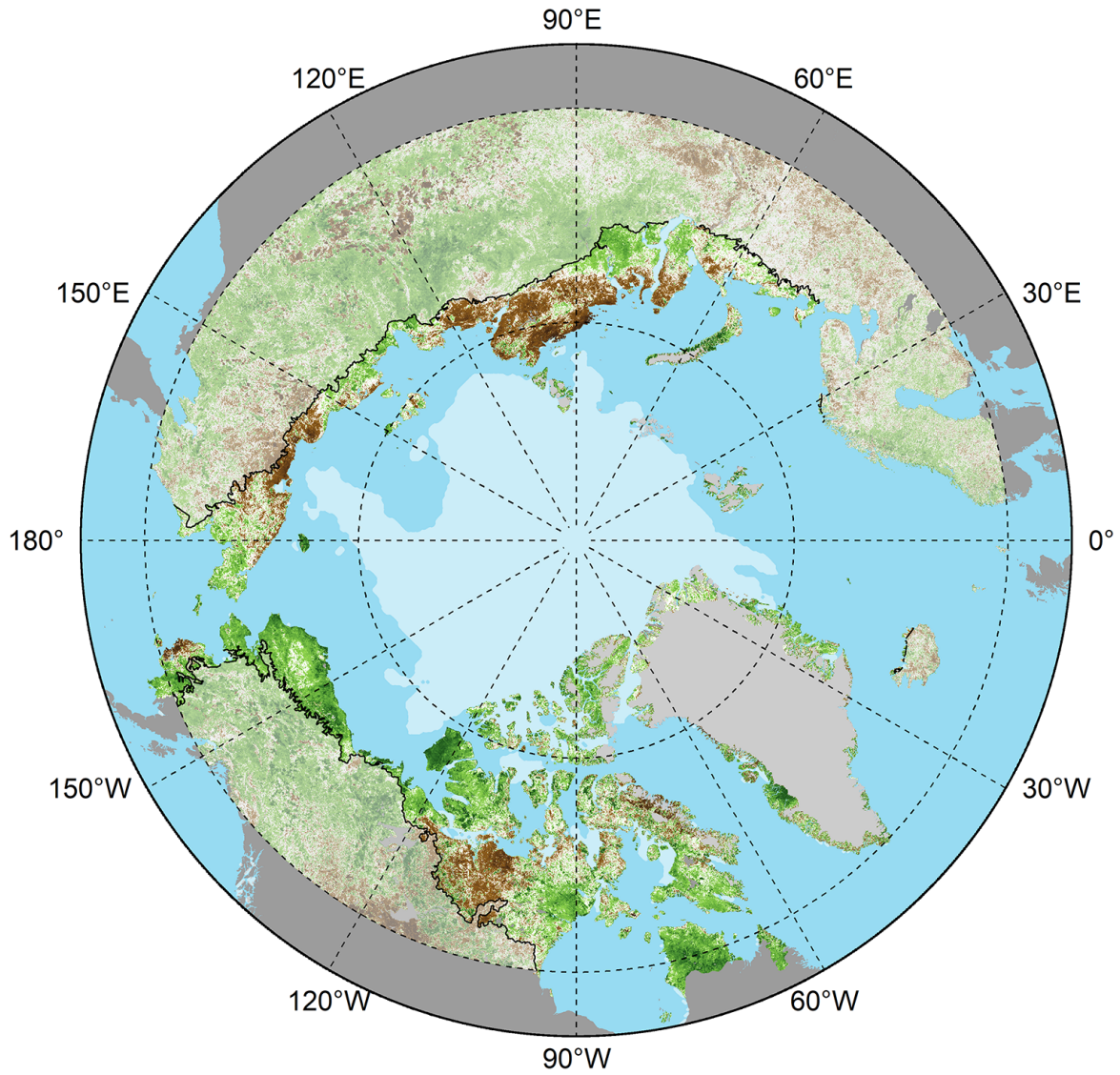


Fig. 2. Time-series of mean MaxNDVI for Arctic tundra from the MODIS MCD13A1 v6.1 (2000-23) dataset for the Eurasian Arctic (red), North American Arctic (blue), and the circumpolar Arctic (black), and from the long-term AVHRR GIMMS-3g+ dataset (1982-2022) for the circumpolar Arctic (gray).

In 2023, the circumpolar MODIS-observed MaxNDVI value increased slightly (0.3%) from the previous year and represents the third highest value in the 24-year MODIS record (Fig. 2). Tundra greenness was much higher than normal across most of the North American Arctic and especially in the Beaufort Sea region, but not in Eurasia, particularly in the East Siberian Sea region where sea ice persisted for much of the summer (Fig. 3). The overall trend in MODIS-observed circumpolar MaxNDVI remains strongly positive, with four of the five highest values in the 24-year record occurring in the last four years (Fig. 2).



MCD13A1 2023 MaxNDVI Anomaly (unitless, compared to 2000–2023 Mean)

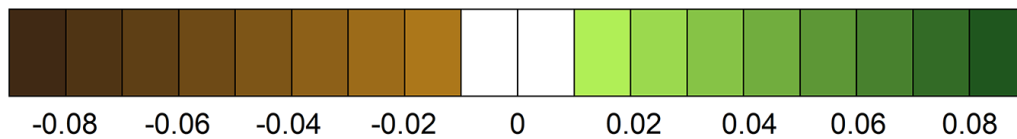


Fig. 3. Circumpolar MaxNDVI anomalies for Arctic tundra (solid colors), and boreal forest north of 60° latitude (muted colors) for the 2023 growing season relative to mean values (2000-23) from the MODIS MCD13A1 v6.1 dataset. The circumpolar treeline is indicated by a black line and the 15 August 2023 sea-ice extent is indicated by light shading.

Drivers and consequences of Arctic greening

Although the underlying drivers of Arctic greening vary from place to place, a growing body of observations brings into focus the types of change that an observer might see on the ground. One of the most widely studied manifestations of Arctic greening is *shrubification*—an increase in the cover, height, and biomass of tundra shrubs such as willows, birches, and alders (Fig. 4) (Mekonnen et al. 2021), largely at the expense of lichens and mosses, which have lower NDVI values (Erlandsson et al. 2023).

Shrubification is also one of the most prevalent forms of change identified by Arctic residents, with consequences for wildlife abundance and human subsistence.



Fig. 4. Arctic landscapes present a complex mosaic of vegetation and waterbodies, which create variability in greenness trends across spatial scales (upper left; Seward Peninsula, Alaska). The expansion of shrubs, such as diamondleaf willow (*Salix pulchra*), is a key long-term driver of Arctic greening (upper right; Mulgrave Hills, Alaska), while ecological disturbances related to permafrost thaw (lower left; Noatak National Preserve, Alaska) and tundra wildfire (lower right; Kanuti River drainage, Alaska) can trigger abrupt declines in greenness at local scales. Photos by G. V. Frost (upper row and lower right) and M. J. Lara (lower left).

Although the satellite record provides unequivocal evidence of widespread tundra greening, there is substantial regional variability in trends that is likely driven by finer-scale, local patterns of vegetation cover and change. Some Arctic regions exhibit little or no trend, while a few, such as the East Siberian Sea sector, exhibit widespread declines, which are thought to reflect ground subsidence and increased surface water triggered by recent permafrost thaw and spring flood events (Magnússon et al. 2023).

Arctic animals can also influence vegetation greenness. For example, in northwestern Siberia, decadal evidence from MODIS and detailed ground-level migration data link herbivory by large semi-domesticated reindeer herds with lower coverage of deciduous shrubs (Spiegel et al. 2023).

While NDVI is typically observed from space, it can also be measured on the ground in tandem with detailed vegetation surveys, providing valuable local context for the trends observed by satellites. For example, Huemrich et al. (2023) compared ground-based NDVI measurements from circa 2001 and 2022 along a transect near Utqiagvik, Alaska. They found that field-measured NDVI trends largely mirrored greening trends detected by MODIS, and were accompanied by increases in leaf area, particularly in wet portions of the landscape.

Arctic greenness trends are influenced by a complex set of interacting climatic and environmental drivers. In the big picture, circumpolar tundra productivity has generally tracked climatic warming over multiple decades. However, the dynamics evident in satellite time-series also reflect many sources of interannual and decadal variability. For example, large-scale atmospheric patterns, such as the Arctic Oscillation and Arctic Dipole, have cascading effects on oceanic circulation, sea-ice extent, and surface air temperatures that influence tundra productivity (Polyakov et al. 2023). These cascading effects create complexity in Arctic greenness trends that operate against the backdrop of long-term climatic warming and sea-ice decline.

Methods and data

The satellite record of Arctic tundra greenness began in late 1981 using AVHRR, a sensor that collects daily observations and continues to operate onboard polar-orbiting satellites. As of September 2023, however, processed AVHRR data were only available through the 2022 growing season. Therefore, we also report observations from the Moderate Resolution Imaging Spectroradiometer (MODIS), a more modern sensor that became operational in 2000. The long-term AVHRR dataset analyzed here for 1982-2022 is the Global Inventory Modeling and Mapping Studies 3g V1.2 dataset (GIMMS-3g+), which is based on corrected and calibrated AVHRR data with a spatial resolution of about 8 km (Pinzon et al. 2023). For MODIS, we computed tundra greenness trends for 2000-23 at a much higher spatial resolution of 500 m, combining 16-day Vegetation Index products from Terra (MOD13A1, version 6.1) and Aqua (MYD13A1, version 6.1) (Didan 2021a,b), referred to here as MCD13A1. Circumpolar maps depicting greenness trends cover the Arctic tundra biome, as well as boreal forest and non-Arctic tundra above 60° N latitude. Time-series plots are based solely on tundra environments within the extent of the Circumpolar Arctic Vegetation Map (Raynolds et al. 2019). MODIS data were further masked to exclude permanent water based on the 2015 MODIS Terra Land Water Mask (MOD44W, version 6). We summarize the GIMMS-3g+ and MODIS records for Maximum NDVI (MaxNDVI), the peak yearly value that is typically observed during the months of July and August.

Acknowledgments

We thank J. Pinzon at the Biospheric Sciences Laboratory, NASA Goddard Space Flight Center for providing updates for the GIMMS-3g+ dataset.

References

- Bartsch, A., and Coauthors, 2021: Expanding infrastructure and growing anthropogenic impacts along Arctic coasts. *Environ. Res. Lett.*, **16**, 115013, <https://doi.org/10.1088/1748-9326/ac3176>.
- Berner, L. T., and S. J. Goetz, 2022: Satellite observations document trends consistent with a boreal forest biome shift. *Global Change Biol.*, **28**(10), 3275-3292, <https://doi.org/10.1111/gcb.16121>.
- Didan, K., 2021a: MODIS/Terra Vegetation Indices 16-Day L3 Global 500m SIN Grid V061 [Data set]. NASA EOSDIS Land Processes Distributed Active Archive Center, <https://doi.org/10.5067/MODIS/MOD13A1.061>.
- Didan, K., 2021b: MODIS/Aqua Vegetation Indices 16-Day L3 Global 500m SIN Grid V061 [Data set]. NASA EOSDIS Land Processes Distributed Active Archive Center, <https://doi.org/10.5067/MODIS/MYD13A1.061>.
- Erlandsson, R., M. K. Arneberg, H. Tømmervik, E. A. Finne, L. Nilsen, and J. W. Bjerke, 2023: Feasibility of active handheld NDVI sensors for monitoring lichen ground cover. *Fungal Ecol.*, **63**, 101233, <https://doi.org/10.1016/j.funeco.2023.101233>.
- Foster, A. C., and Coauthors, 2022: Disturbances in North American boreal forest and Arctic tundra: impacts, interactions, and responses. *Environ. Res. Lett.*, **17**, 113001, <https://doi.org/10.1088/1748-9326/ac98d7>.
- Heijmans, M. M. P. D., and Coauthors, 2022: Tundra vegetation change and impacts on permafrost. *Nat. Rev. Earth Environ.*, **3**, 68-84, <https://doi.org/10.1038/s43017-021-00233-0>.
- Huemmrich, K. F., J. Gamon, P. Campbell, M. Mora, S. Vargas Z, B. Almanza, and C. Tweedie, 2023: 20 years of change in tundra NDVI from coupled field and satellite observations. *Environ. Res. Lett.*, **18**, 094022, <https://doi.org/10.1088/1748-9326/acee17>.
- Magnússon, R. Í., F. Groten, H. Bartholomeus, K. van Huissteden, and M. M. P. D. Heijmans, 2023: Tundra browning in the Indigirka Lowlands (north-eastern Siberia) explained by drought, floods and small-scale vegetation shifts. *J. Geophys. Res.-Biogeosci.*, **128**, e2022JG007330, <https://doi.org/10.1029/2022JG007330>.
- Mekonnen, Z. A., and Coauthors, 2021: Arctic tundra shrubification: a review of mechanisms and impacts on ecosystem carbon balance. *Environ. Res. Lett.*, **16**, 053001, <https://doi.org/10.1088/1748-9326/abf28b>.
- Pinzon, J. E., E. W. Pak, C. J. Tucker, U. S. Bhatt, G. V. Frost, and M. J. Macander, 2023: Global Vegetation Greenness (NDVI) from AVHRR GIMMS-3G+, 1981-2022 [Data set]. ORNL DAAC, Oak Ridge, TN, USA, <https://doi.org/10.3334/ORNLDAAC/2187>.
- Polyakov, I. V., R. B. Ingvaldsen, A. V. Pnyushkov, U. S. Bhatt, J. A. Francis, M. Janout, R. Kwok, and Ø. Skagseth, 2023: Fluctuating Atlantic inflows modulate Arctic atlantification. *Science*, **381**, 972-979, <https://doi.org/10.1126/science.adh5158>.

Raynolds, M. K., and Coauthors, 2019: A raster version of the Circumpolar Arctic Vegetation Map (CAVM). *Remote Sens. Environ.*, **232**, 111297, <https://doi.org/10.1016/j.rse.2019.111297>.

Rogers, A., S. P. Serbin, and D. A. Way, 2022: Reducing model uncertainty of climate change impacts on high latitude carbon assimilation. *Global Change Biol.*, **28**, 1222-1247, <https://doi.org/10.1111/gcb.15958>.

Spiegel, M. P., A. Volkovitskiy, A. Terekhina, B. C. Forbes, T. Park, and M. Macias-Fauria, 2023: Top-down regulation by a reindeer herding system limits climate-driven Arctic vegetation change at a regional scale. *Earth's Future*, **11**, e2022EF003407, <https://doi.org/10.1029/2022EF003407>.

Mention of a commercial company or product does not constitute an endorsement by NOAA/OAR. Use of information from this publication concerning proprietary products or the tests of such products for publicity or advertising purposes is not authorized. Any opinions, findings, and conclusions or recommendations expressed in this material are those of the authors and do not necessarily reflect the views of the National Oceanic and Atmospheric Administration.

November 12, 2023